

Renormalization group analysis of graphene-phosphorene van der Waals heterostructure

Sushant Kumar Behera and Pritam Deb*

*Advanced Functional Material Laboratory, Department of Physics,
Tezpur University (Central University), Tezpur-784028, India.*

(Dated: June 8, 2022)

Weak-coupling phenomena of the two-dimensional Hubbard model is gaining momentum as a new interesting research field due to its extraordinarily rich behavior as a function of the carrier density and model parameters. Thus, there is a rapidly growing interest in the transmission of information encoded by electron and atomic spins which, in principle, can be realized by the propagation of spin waves through low-dimensional sheets. In this paper, we demonstrate the spin-wave dependent electronic structure and susceptibility behavior of model graphene-phosphorene van der Waals heterostructure in the framework of renormalization group (RG) approach. We implement Aharonov-Bohm-Coulomb-Dirac formulated field-theoretic approach for the weakly interacting Fermi system with nearest-neighbor hopping amplitudes. The analytical approach is further extended for spin-wave dependent susceptibility behavior. This finding supports the quantitative realization of experimental and theoretical systems further from their critical points before the underlying field theory is well understood for potential application.

keywords: Renormalization group theory; two dimensional van der Waals heterostructure; weakly interacting Fermi system; spin-wave dependent susceptibility; Vertex response function

I. INTRODUCTION

Correlation effects in condensed matter many-body systems could be fundamentally described *via* Hubbard model [1–10]. It exhibits various different channels for the transition of normal metallic behavior by an independent tunability of the electronic band structure *via* a single tight-binding parameter, *i.e.*, the inter-layer hopping amplitude, and the half-filling nature on the hexagonal lattice bilayer system. In this aspect, weak-coupling phenomena of the two-dimensional (2D) Hubbard model is gaining momentum as a new interesting research field recently because of its extraordinarily rich behavior as a function of the carrier density and model parameters. Renormalization Group method is presently the most promising and best controlled analytical approach to low dimensional Fermi systems with competing singularities at weak coupling region *via* Aharonov-Bohm field potential. In this regard, theoretical investigation of spin-wave propagation through van der Waals (vdW) heterostructure provides suitable platform to explore the concept of spin-wave assisted field effect transistor in molecular spintronic [11]. In this aspect, atomically thin 2D materials, like hexagonal-boron nitride (h-BN), graphene (Grp) and its family, transition metal dichalcogenides (TMDCs), black phosphorous (BP), etc. cover interesting field of research because of their rich mechanical [1–3], electronic [4, 5], optical [6, 7] and electrochemical assets with an extensive variety of promising applications [8–10]. In recent times, multilayer vdWs heterostructures, chemically different 2D structures, have attracted recent research attention

unlike monolayer pristine systems, like Grp/h-BN [12], Grp/TMDC [13], h-BN/TMDC [14], Grp/Silicene [15] and TMDC/TMDC [16]. While, many 2D materials (*e.g.* graphene and MoS₂) with efficient carrier mobilities (*i.e.* high *on-off* ratio) [17, 18] restrict their nano-dimension heterolayer device applications. In these case, these layered 2D vdW heterostructures possess superior efficiency for carrier inoculation *via* barrier height modulation [19]. In this regard, phosphorene (P), a puckered honeycomb 2D material, possesses fascinating electronic and optical properties, such as finite direct band gap (~ 1.5 eV at monolayer) and high mobility ($10^3 \text{ cm}^2 \text{ V}^{-1} \text{ s}^{-1}$ at 300 K) due to its structural anisotropy [20–25].

To analyze prototypic 2D model for the electronic degrees of freedom, Hubbard model including Renormalization Group (RG) theory is promising in case of 2D planes [26]. In particular, 2D Hubbard model is appropriate to explain interesting phenomena of weakly interacting systems which can be tuned by their carrier density. Besides, large scale numerical algorithms are worked out to solve such 2D interacting Hubbard model including related model parameters [27]. In such systems, weak interaction reveals antiferromagnetic ground state close to half-filling and symmetric *s*-wave phase away from half-filling region. In such cases, conventional perturbation theory fails at a certain region close to the half-filling region, where challenging and frequent infrared deviations raise due to weakly interacting Fermion system [28–30] and *van Hove singularities* [31] including the Aharonov-Bohm (AB) potential field for 2D graphene monolayer system [32–34]. Moreover, theoretical model of 2D weakly interacting Fermi systems having challenging singularities near weakly interacting region is still lacking in the current analytical prospects

* Corresponding Author: pdeb@tezu.ernet.in

for vdW heterostructures. Thus, RG theory is presently the most promising and well-ordered technique for such 2D weakly interacting Fermi systems [35, 36].

In the present manuscript, we implement RG theory to the 2D Hubbard model of Graphene-Phosphorene (Grp-P) heterostructure considering nearest neighbor hopping amplitudes of dense electron distribution profile close to half-filling region. Here, we particularly calculate the trend of collective two particle couplings in a single loop stage, completely ignoring the inappropriate energy and linear momentum dependency, but considering vital tangential momentum dependency being a dynamic parameter. We further extend the RG theory to obtain the susceptibility values to analyze the physical response of uncertainties gestured by diverging couplings in weakly interacting vdW heterostructure. Charge-density, spin-density and singlet function based susceptibilities have been considered during analytical calculations at various pairing symmetries. Here, spin-density phase diagram has been presented close to half-filling region of this 2D Hubbard model. The obtained results show the critical energy scale behavior away from the half-filling region with perfect nesting and room temperature stability of the designed system for further functionality. The rest of this manuscript is organized as follows: The methodology details covering the field-theoretic formulation and renormalization group approach are given in Section II and Section III, respectively. We present details of the obtained results and corresponding discussions of vertex function findings in Section IV. Lastly, the conclusions of this manuscript are summarized in Section V.

II. FIELD THEORY FRAMEWORK

The Hamiltonian with the order of second quantization (H_{SQ}) [37] unfolding the massless 2D Dirac fermions is referred below, as

$$H_{SQ} = \int dv \xi^\dagger(v) [v_F [-i\hbar \nabla + eA(v)] \sigma - eV(v)] \xi(v) \quad (1)$$

where, e , σ , v_F and ξ^\dagger are the electron charge, spin-wave projection, Fermi velocity and Grassmann variable, respectively. The Coulomb field potential originated due to the net charge of Ze positioned at the origin is $V(v) = \frac{Ze}{4\pi\epsilon_0 v}$, similarly the AB field solenoid aligned at

the same point provides $A(v) = \frac{\Phi}{2\pi} (-\frac{y}{v^2}, \frac{x}{v^2})$ with a fixed total magnetic flux of Φ . Being the fixed magnetic flux, Pearl's substitution approach is limited in the flow equation. This establishes the Aharonov-Bohm-Coulomb-Dirac (ABCD) field problem in the present model 2D

vdW heterostructure [38].

The partial wave expansion can be further expanded using rotational symmetry, which decouples the system Hamiltonian into diverse partial-wave vectors. Here, $j=(1/3), (3/2), \dots$ is the net angular momentum and we consider the dimension-free Coulomb field coupling, $C = \frac{Ze^2}{4\pi\epsilon_0 \hbar v_F}$. Apart from the kinetic term, each radical Hamiltonian contains the Coulomb field potential and the centrifugal field potential, both of them possess scale-invariant form (*i.e.* $1/v$). Most interesting physical quantities are the charge density $\rho(v) = -e \langle \xi^\dagger v \xi(v) \rangle$ and current density $J(v) = -ev_F \langle \xi^\dagger v \sigma \xi(v) \rangle$ in the ground state of the ABCD Hamiltonian equation. The corresponding coupling presents scattering amplitude located at potential center and corresponding energy dependency is to be obtained using RG equations.

III. RENORMALIZATION GROUP THEORY

We have taken weakly interacting spin-half Fermions of single-particle basis state with crystal momentum (k_c), *up* or *down* spin-wave projection, $\sigma \in [\uparrow, \downarrow]$ and kinetic energy (E_k). Thus, the behavioral aspects of the system can be determined via following equation,

$$S[\xi, \xi'] = \sum_K (i f_0 - \xi_K) \xi'_K \xi_K - \gamma[\xi, \xi'] \quad (2)$$

where, $K=(f_0, k, \sigma)$ presents a multi index parameter connecting the frequency (f_0) with each particle quantum numbers; Grassmann variables (ξ_K and ξ'_K) are allied to the formation and extinction operators, $\xi_K = \epsilon_K - \mu$ is the energy related to a particle depending on the chemical potential (μ) and $\gamma[\xi, \xi']$ is a random many body coupling factor [39, 40].

Here, all the connected flow equations via Green functions can be achieved from the functional which is used for their generation, given below

$$G[\eta, \eta'] = \log \int \partial \mu_c[\xi, \xi'] e^{-\gamma[\xi, \xi']} e^{(\xi', \eta) + \xi, \eta'} \quad (3)$$

with the normalized Gaussian measure.

The infinite hierarchy in flow equations is essential to check at a single-loop level to predict dominant structural uncertainties in the vdW system within weakly interacting limit, neglecting other irrelevant components of the effective interactions. Moreover, energy corrections of each iteration step are confined to one-particle vertex function (Γ) and used for further calculations. The spin-wave structure of Γ can be used for a spin rotation invariant system with response flow equation, which is given as follow,

$$\Gamma(K'_1, K'_2; K_1, K_2) = \Gamma_s(K'_1, K'_2; K_1, K_2) \Lambda^{1/2} S_{\sigma'_1, \sigma'_2; \sigma_1, \sigma_2} + \Gamma_t(K'_1, K'_2; K_1, K_2) \Lambda^{3/2} T_{\sigma'_1, \sigma'_2; \sigma_1, \sigma_2} \quad (4)$$

where, K_1 and K_2 presents the multi indexed particle quantum numbers for both spin arrangements, singlet S and triplet T projection operators are used for two particle spin space, Λ is the energy scale varying at a functional trend for singlet and triplet operators.

We extend the RG equations to obtain linear response behaviour (*i.e.* spin-wave susceptibility value) of the system towards finite applied external electric field [41]. Finite external field (F_E) leads to an additional contribution to the action of the flow equation, which is given as follow

$$\zeta[F_E; \xi, \xi'] = - \sum_q [F'_E(q)\Phi(q) + F_E(q)\Phi'(q)] \quad (5)$$

Here, the Grassmann variables in bilinear form ($\Phi(q)$), Hermitian conjugate ($\Phi'(q)$) and $F'_E(q)$ is the complex conjugate of $F_E(q)$. One can calculate the response of the field interaction towards electronic charge density, $\rho(q) = \sum_{k,\sigma} (\xi'_{k-q,\sigma} \xi_{k,\sigma})$ and z-direction dependent spin density, $s^z(q) = \sum_k [\xi'_{k-q,\uparrow} \xi_{k,\uparrow} - \xi'_{k-q,\downarrow} \xi_{k,\downarrow}]$ and response to coupling fields which interact with the change in singlet operator, where $\partial(k)$ is an even parity function satisfying the orbital symmetry of the coupling operator (*i.e.* s wave). The linear response of the expectation value with the flow equation of the partition function $[F_E]$. Here, the susceptibility follows like,

$$\chi(q) = \xi^{-1} \langle \Phi(q)\Phi'(q) \rangle_{F_E=0} \quad (6)$$

Here, translation and spin rotation invariant systems are considered with conserved charge in the absence of an external field (F_E). Here, in such normal and non-symmetrical broken phase, $\langle \Phi(q) \rangle$, the expectation value nullifies at $F_E(q) \rightarrow 0$.

IV. VERTEX FUNCTION FINDINGS

The ow of the vertex function (Γ) and the susceptibility (χ) values have been calculated analytically using RG theory for several choices of the bare interaction, termed as the AB field potential ($U_i(0)$), the next nearest neighbor hopping amplitude ($t_i(0)$) and the chemical potential (μ), where t and μ have been fixed so that the Fermi surface and particle density are approaching to ε_k and half-filling (*i.e.* $n \simeq 1$, $\mu \rightarrow 0$), respectively. Momentum dependent flow of the vertex functions are obtained for the three considered systems at low dimensional scale. It is observed that the flow of the vertex function achieves a density value ($n \simeq 0.992$), *i.e.* close to half-filling region at $t=0$ and $\mu=0.005$ (plotted in Figure 1). Here, the singlet part of the vertex function is taken at specified values of momenta on the Fermi surface including the values of momenta, where strong renormalization of Γ occurs. Most probably, the singlet vertex function possesses its leading values supporting *umklapp* scattering along the diagonal direction of the k -space Brillouin zone. It is observed from the RG theory calculation that the density decreases away from

half-filling (*i.e.* $n \simeq 1$, $\mu \rightarrow 0$) region in a step-like manner and the calculations fail into a region, where s -wave symmetry dominates with pairing correlations at necessarily low scale energy levels indicating quantum confinement (*i.e.* nanostructuring) in the Grp-P heterostructure system.

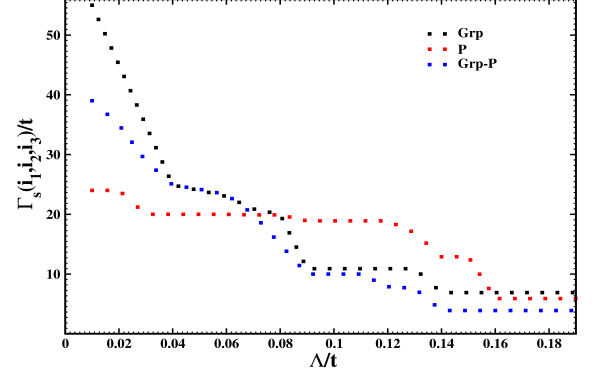


FIG. 1. Flow of the singlet vertex function, Γ , as a function of Λ for several selections of momenta values, k_{F1} , k_{F2} and k_{F3} .

Two types of antiferromagnetic spin-wave (*i.e.* incommensurate and commensurate) susceptibilities have been obtained from the numerical calculations to validate the physical instability associated with the diverging vertex function as a consequence of response functions [42–45]. It is observed that the incommensurate spin susceptibilities can be neglected compared to their respective commensurate counterparts (shown in Figure 2) due to the incommensurability parameter ($\delta \sim 0$) nearing to half-filling (*i.e.* $n \simeq 1$, $\mu \rightarrow 0$) as a function of energy scale. Moreover, the ratios between the two susceptibility values of monolayer system in case of weakly interacting s -wave region are in the same scale, whereas the ratios of free susceptibility are much reduced indicating the validity of response functions for 2D weakly coupled Fermi systems. In addition, the ratio in case of hetero bilayer is much greater compared to its monolayer system. Thus, antiferromagnetic wave vector based spin-wave susceptibility dominates over coupled susceptibilities at low scale energy level (*i.e.* ground state), confirming the existence of antiferromagnetic ground state with rotational spin invariance.

We show the phase diagram of μ and U at half-filling measured by the prevailing uncertainty from the flow equation (shown in Figure 3(a)). The leading uncertainty region in case of commensurate spin-wave density is detached from the s -wave coupling region *via* a narrow strip where incommensurate spin-wave density fluctuations show dominant effect with $q=(\pi, \pi-\delta)$. For small value of U , the region surrounding half-filling is exponentially small, where uncertainties in spin-wave density play a dominant effect. The value of (t , U), in-plane

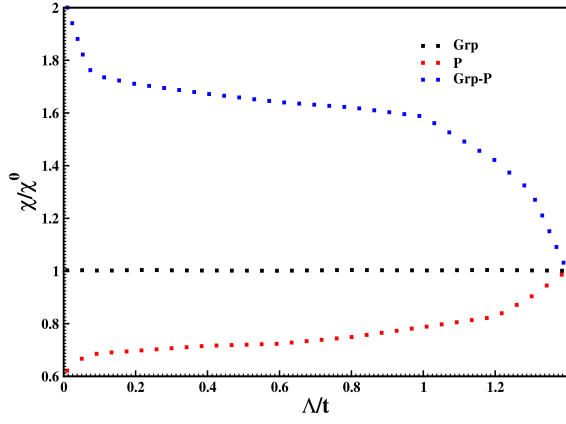


FIG. 2. The flow of the ratio of weakly interacting and free susceptibility values depending on Λ values for the three systems. The model parameters are $U=t$ and $t=0$, and the chemical potential $|\mu|=0.005$.

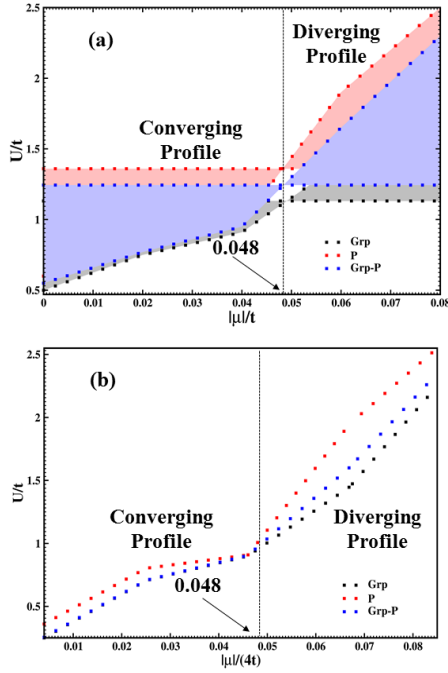


FIG. 3. The (μ, U) phase diagram for $t=0$ close to half-filling ($n=1, |\mu| \rightarrow 0$) region; the solid line represents the spin-density-wave regime. (b) The (t, U) phase diagram for $4t \neq 0$ value below the half-filling ($|\mu| \neq 0$) region; the dotted lines represent the spin-density-wave regime.

phase diagram is shown in Figure 3(b) with $|\mu|=4t$ and $\mu \neq 0$ (below half-filling). It is observed that the chemical potential is fixed at the van Hove singularity [46] irrespective of the value of spin-wave density, which is decreasing away from half-filling region with growing value of $|\mu|$ at 0.048, one critical point in the flow equation.

The behavioral trend of critical energy scale, Λ_c , depending on the function at $t \neq 0$ where, $|\mu| \rightarrow 0$ and $U=t$ is plotted in Figure 4(a). The shrinkage in the

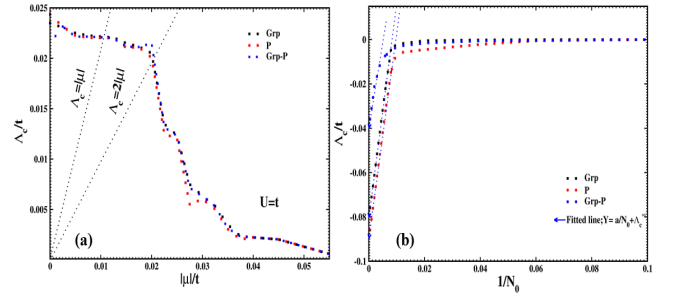


FIG. 4. The critical energy scale, Λ_c , as a function of (a) μ at $U=t$ and $n=1$. The dotted black lines present the functions for $\Lambda_c = |\mu|$ and $\Lambda_c = 2|\mu|$. (b) number of discretization points, N_0 , upon Fermi surface at $U=t$, $n=1$ and $|\mu|=0.005$. The dotted black lines represent the functions $Y = a/(N_0 + \Lambda_c)$. The flow of (c) compressibility, κ , and (d) homogeneous spin susceptibility as a function of Λ at fixed value of $|\mu|=0.005$ for $U=t$ and $n=1$.

value of Λ_c with growing trend of $|\mu|$ confirms that the E_F resides on the *van Hove singularity* within the weakly interacting regime having only Fermi surface nesting dominance. Momentum variables of Γ have been projected upon the Fermi surfaces at specific points, where the strong renormalization of the vertex function occurs. Here, total 8 fixed points considered for the normalization process. Besides, additional 8 points have been considered in a more refined projection scheme upon the *van Hove surface* to check the collective effect. As a result, sum total 16 points (8 for *Fermi surface* and 8 for *van Hove surface*) have been taken during the flow equation calculations. These refinements, in the response function of the spin-wave density scheme, enhance the analytical calculation efficiency significantly with a reasonable reduction in critical energy scale, without altering Γ and χ values, qualitatively. The variation trend of Λ_c as a function of the inverse number of discretization points, N_0 , upon the Fermi surface at fixed choice of model parameters is shown in Figure 4(b). It is noticed that the critical energy scale is varying in a discrete manner with 8 discretization points, and resumes stability for next 8 points with right order of magnitude indicating the controlled trend of flow equation for weakly interacting systems.

The values of compressibility and homogeneous spin susceptibility have been calculated depending on the energy scale (shown in Figure 5(a) and (b)), respectively for the three systems. These two parameters can be realized directly from the forward scattering of vertex function *via* Landau equations of Fermi-liquid theory [47]. The free compressibility, k_0 , and spin-wave susceptibility, $\chi(s,0)$, are refined ignoring infrared cut-off values as per the Fermi-Liquid theory. As a result, the flow equations of the vertex response function is entirely stable because of the flow of the Landau functions at the initial stage of the normal random phase approximation of the

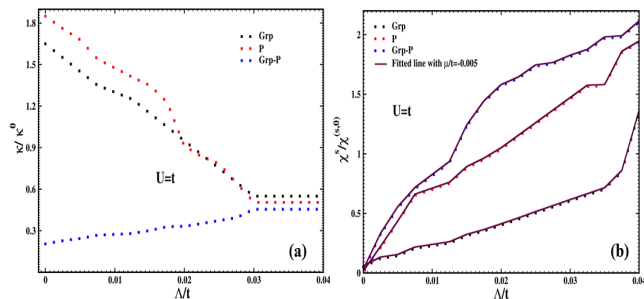


FIG. 5. The flow of (a) compressibility, κ , and (b) homogeneous spin susceptibility as a function of Λ at fixed value of $\mu = 0.005$ for $U=t$ and $n=1$.

Hubbard model at critical energy scale value, $\Lambda = \Lambda_c$. The compressibility is inhibited at low scale energy levels close to half-filling region, which is expected for systems having a finite bandgap near to μ , with dominant uncertainty in spin-wave density. Besides, the values of the compressibility diverge with respect to the reduction in homogeneous spin-wave susceptibility values away from half-filling region, where s -wave uncertainties play major role acting indicating a finite spin-wave bandgap opening trend in any singlet or triplet spin-wave 2D Fermi systems [48]. It is found that the spin-wave susceptibility flows from zero to negative values which implies that our single loop calculation fails, when it reaches strongly interacting regime. This trend is validated only in weakly interacting region applied for 2D Fermi system. Thus, one diverging compressibility is found mentioning a strong tendency toward phase transition and separation. As a result, the increase of k sets is very close to the uncertainty, where the renormalized interactions achieve large value that the single loop findings are not further validated. The stability is prominent at higher energy scales (*i.e.* $0.04 \leq \frac{\Lambda}{t} \leq 0.03$) from the plot in Figure 5((a) and (b)). Moreover, we

have shown the trend of free susceptibilities (χ_0) at specific choice of t and μ values (shown in supplementary information Figures S1) which is strongly supporting the trend of homogeneous spin-wave susceptibility.

V. SUMMARY AND CONCLUSIONS

A study on the spin-wave response function behavior of vdW Grp-P heterostructure was presented via field-theory perspective implementing analytical RG method. This formulation can be used systematically to identify coupling uncertainties in 2D weakly interacting Fermi systems. In this system, critical energy can be scaled at specific singular points where vertex functions and susceptibilities diverge and become finite. Moreover, the instabilities are modulated via short range antiferromagnetic correlations present in the system, which is noticed from the ow of vertex functions and susceptibilities. This antiferromagnetic ordering is retained in the ground state of such 2D systems accompanied with rotational spin invariance. The analytical results show an unusual singularity of van Hove kind in 2D heterostructure. This finding supports the quantitative realization of experimental and theoretical systems further from their critical points and before the underlying field theory is well understood. This will also facilitate quantitative analysis of room temperature stability of such systems and *on-state* modeling of electronic devices in future.

ACKNOWLEDGMENTS

SKB acknowledges DST, Govt. of India for providing INSPIRE Fellowship (IF150325). The authors acknowledge Tezpur University for providing HPCC facility.

-
- [1] Y. Nishida, Phys. Rev. B **94**, 085430 (2016).
 - [2] A. Raju, C. B. Clement, L. X. Hayden, J. P. Kent-Dobias, D. B. Liarte, D. Z. Rocklin, and J. P. Sethna, Phys. Rev. X **9**, 021014 (2019).
 - [3] A. K. Geim, Science **324**, 1530 (2009).
 - [4] Y. Cai, G. Zhang, and Y.-W. Zhang, Journal of the American Chemical Society **136**, 6269 (2014).
 - [5] Y. Zhang, J. P. Small, M. E. S. Amori, and P. Kim, Phys. Rev. Lett. **94**, 176803 (2005).
 - [6] S. Qian, X. Sheng, X. Xu, Y. Wu, N. Lu, Z. Qin, J. Wang, C. Zhang, E. Feng, W. Huang, and Y. Zhou, J. Mater. Chem. C **7**, 3569 (2019).
 - [7] M. Fan, J. Wu, J. Yuan, L. Deng, N. Zhong, L. He, J. Cui, Z. Wang, S. K. Behera, C. Zhang, J. Lai, B. I. Jawdat, R. Vajtai, P. Deb, Y. Huang, J. Qian, J. Yang, J. M. Tour, J. Lou, C.-W. Chu, D. Sun, and P. M. Ajayan, Advanced Materials **31**, 1805778 (2019).
 - [8] Y.-C. Rao, S. Yu, and X.-M. Duan, Phys. Chem. Chem. Phys. **19**, 17250 (2017).
 - [9] N.-N. Zhang, C. Sun, X.-M. Jiang, X.-S. Xing, Y. Yan, L.-Z. Cai, M.-S. Wang, and G.-C. Guo, Chem. Commun. **53**, 9269 (2017).
 - [10] S. K. Behera and P. Deb, Phys. Chem. Chem. Phys. **20**, 26688 (2018).
 - [11] S. Z. Butler, S. M. Hollen, L. Cao, Y. Cui, J. A. Gupta, H. R. Gutierrez, T. F. Heinz, S. S. Hong, J. Huang, A. F. Ismach, E. Johnston-Halperin, M. Kuno, V. V. Plashnitsa, R. D. Robinson, R. S. Ruoff, S. Salahuddin, J. Shan, L. Shi, M. G. Spencer, M. Terrones, W. Windl, and J. E. Goldberger, ACS Nano **7**, 2898 (2013).
 - [12] S. K. Behera and P. Deb, RSC Adv. **7**, 31393 (2017).
 - [13] S. K. Behera, P. Deb, and A. Ghosh, ChemistrySelect **2**, 3657.

- [14] Z. Huang, C. He, X. Qi, H. Yang, W. Liu, X. Wei, X. Peng, and J. Zhong, *Journal of Physics D: Applied Physics* **47**, 075301 (2014).
- [15] M. F. Bhopal, D. W. Lee, A. u. Rehman, and S. H. Lee, *J. Mater. Chem. C* **5**, 10701 (2017).
- [16] G. Mills and H. Jónsson, *Phys. Rev. Lett.* **72**, 1124 (1994).
- [17] A. H. Castro Neto, F. Guinea, N. M. R. Peres, K. S. Novoselov, and A. K. Geim, *Rev. Mod. Phys.* **81**, 109 (2009).
- [18] M. Y. Han, B. Özyilmaz, Y. Zhang, and P. Kim, *Phys. Rev. Lett.* **98**, 206805 (2007).
- [19] Y. Cai, G. Zhang, and Y.-W. Zhang, *The Journal of Physical Chemistry C* **119**, 13929 (2015).
- [20] N. D. Mermin and H. Wagner, *Phys. Rev. Lett.* **17**, 1133 (1966).
- [21] J. Yuan, S. Najmaei, Z. Zhang, J. Zhang, S. Lei, P. M. Ajayan, B. I. Yakobson, and J. Lou, *ACS Nano* **9**, 555 (2015).
- [22] H. Liu, A. T. Neal, Z. Zhu, Z. Luo, X. Xu, D. Tomnek, and P. D. Ye, *ACS Nano* **8**, 4033 (2014).
- [23] R. W. Keyes, *Phys. Rev.* **92**, 580 (1953).
- [24] M. Talukdar, S. K. Behera, K. Bhattacharya, and P. Deb, *Applied Surface Science* **473**, 275 (2019).
- [25] Y. Shi, W. Zhou, A.-Y. Lu, W. Fang, Y.-H. Lee, A. L. Hsu, S. M. Kim, K. K. Kim, H. Y. Yang, L.-J. Li, J.-C. Idrobo, and J. Kong, *Nano Letters* **12**, 2784 (2012).
- [26] Y. Hadad and B. Z. Steinberg, *Phys. Rev. Lett.* **105**, 233904 (2010).
- [27] V. P. Gusynin and S. G. Sharapov, *Phys. Rev. Lett.* **95**, 146801 (2005).
- [28] D. Torelli and T. Olsen, *2D Materials* **6**, 015028 (2018).
- [29] K. G. Wilson, *Rev. Mod. Phys.* **47**, 773 (1975).
- [30] R. Shankar, *Rev. Mod. Phys.* **66**, 129 (1994).
- [31] N. E. Bickers, D. J. Scalapino, and S. R. White, *Phys. Rev. Lett.* **62**, 961 (1989).
- [32] N. E. Bickers, D. J. Scalapino, and S. R. White, *Phys. Rev. Lett.* **62**, 961 (1989).
- [33] A. Kumar, T. Low, K. H. Fung, P. Avouris, and N. X. Fang, *Nano Letters* **15**, 3172 (2015).
- [34] D. Ebert, V. C. Zhukovsky, and E. A. Stepanov, *Journal of Physics: Condensed Matter* **26**, 125502 (2014).
- [35] N. Furukawa, T. M. Rice, and M. Salmhofer, *Phys. Rev. Lett.* **81**, 3195 (1998).
- [36] M. Salmhofer, *Communications in Mathematical Physics* **194**, 249 (1998).
- [37] J. W. Negele and H. Orland, “Quantum many particle systems,” (Addison-Wesley Reading, Massachusetts, 1987).
- [38] M. O. Goerbig, *Rev. Mod. Phys.* **83**, 1193 (2011).
- [39] Y. Aharonov and D. Bohm, *Phys. Rev.* **115**, 485 (1959).
- [40] B. J. Dalton, J. Jeffers, and S. M. Barnett, *Annals of Physics* **370**, 12 (2016), 1604.03375.
- [41] K. E. Newman and E. K. Riedel, *Phys. Rev. B* **25**, 264 (1982).
- [42] M. A. Metlitski and S. Sachdev, *Phys. Rev. B* **82**, 075128 (2010).
- [43] P. Bartlett, R. H. Ottewill, and P. N. Pusey, *Phys. Rev. Lett.* **68**, 3801 (1992).
- [44] S. A. Kivelson, I. P. Bindloss, E. Fradkin, V. Oganessian, J. M. Tranquada, A. Kapitulnik, and C. Howald, *Rev. Mod. Phys.* **75**, 1201 (2003).
- [45] S. Higashitani, *Phys. Rev. B* **89**, 184505 (2014).
- [46] J.-M. Stéphan, S. Furukawa, G. Misguich, and V. Pasquier, *Phys. Rev. B* **80**, 184421 (2009).
- [47] G. Y. Chitov and D. Sénéchal, *Phys. Rev. B* **57**, 1444 (1998).
- [48] V. B. Shenoy, *Phys. Rev. A* **88**, 033609 (2013).